JOURNAL OF NATURAL PRODUCTS

Article

pubs.acs.org/jnp

Antiausterity Agents from *Uvaria dac* and Their Preferential Cytotoxic Activity against Human Pancreatic Cancer Cell Lines in a Nutrient-Deprived Condition

Suresh Awale,*[,†,‡] Jun-ya Ueda,[†,‡] Sirivan Athikomkulchai,[§] Sherif Abdelhamed,[‡] Satoru Yokoyama,[‡] Ikuo Saiki,[‡] and Ryuta Miyatake[⊥]

[†]Frontier Research Core for Life Sciences, University of Toyama, 2630 Sugitani, Toyama 930-0194, Japan

[‡]Institute of Natural Medicine, University of Toyama, 2630 Sugitani, Toyama 930-0194, Japan

[§]Faculty of Pharmacy, Srinakharinwirot University, Nakhon Nayok, 26120, Thailand

[⊥]Graduate School of Science and Engineering, University of Toyama, 3190 Gofuku, Toyama 930-8555, Japan

Supporting Information

ABSTRACT: Human pancreatic cancer cell lines are known for their inherent tolerance to nutrition starvation, which enables them to survive under a hypovascular (austerity) tumor microenvironment. The search for agents that preferentially retard the survival of cancer cells under low nutrition conditions (antiausterity agent) is a novel approach to anticancer drug discovery. In this study, it was found that a dichloromethane extract of the stem of *Uvaria dac* preferentially inhibited PANC-1 human pancreatic cancer cells survival under nutrition-deprived conditions at a concentration of 10 μg/mL. Workup of this bioactive extract led to the discovery of (+)-grandifloracin (**8**) as a potent antiausterity agent as evaluated in a panel of four human pancreatic cancer cell lines, PANC-1 (PC_{50}, 14.5 μM), PSN-1 (PC_{50}, 32.6 μM), MIA PaCa-2 (PC_{50}, 17.5 μM), and KLM-1 (32.7 μM). (+)-Grandifloracin (**8**) has been isolated from a natural source for the first time. Its absolute stereochemistry was established by single-crystal X-ray crystallography and circular dichroism spectroscopic analysis. In addition to this, seven other new highly oxygenated cyclohexene derivatives, named uvaridacanes A (**1**) and B (**2**), uvaridacols A–D (**3**, **4**, **6**, **7**), and uvaridapoxide A (**5**), were also isolated and structurally characterized.

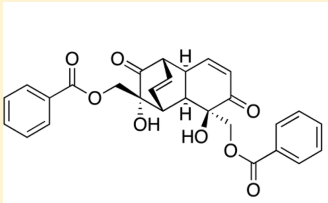

(+)-Grandifloracin (**8**)

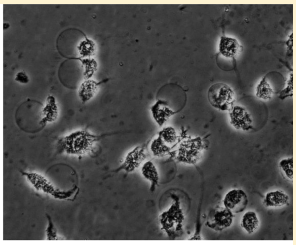

PANC-1 Cell death induced by (+)-grandifloracin (**8**)

The plant *Uvaria dac* Pierre ex Finet & Gagnep belongs to the plant family Annonaceae. This is a woody tree endemic to southeast Asian countries such as Thailand and Vietnam. Locally, it is known as "kluai I hen" in Thailand. A number of other plants belonging to the genus *Uvaria* have been found in many parts of the world and reported to contain acetogenins,[1] polyoxygenated cyclohexenes,[2] benzylated flavanones,[3,4] chalcones,[5] and sesquiterpenes,[6] which possess diverse biological activities such as cytotoxic,[7,8] antibacterial,[9] antimalarial,[10] and antimicrobial[11] effects. Until now, there has been no prior study on the chemical constituents of *U. dac*. In a continued antiausterity strategy-based screening procedure for medicinal plants,[12−20] it was found that a CH_2Cl_2 extract of *U. dac* collected from Thailand showed preferential cytotoxic activity against the PANC-1 human pancreatic cancer cell line at a concentration of 10 μg/mL. Therefore, the chemical constituents were isolated, and nine compounds together with seven new highly oxygenated cyclohexene derivatives, named uvaridacanes A (**1**) and B (**2**), uvaridacols A–D (**3**, **4**, **6**, **7**), and uvaridapoxide A (**5**), were obtained. In addition, (+)-grandifloracin (**8**) was isolated for the first time from a natural source. We report herein the structure of these new compounds together with their preferential cytotoxic activity against a panel of four pancreatic cancer cell lines.

RESULTS AND DISCUSSON

Uvaridacane A (**1**) was isolated as a white, amorphous solid. Its molecular formula was determined by HRFABMS to be $C_{19}H_{18}O_4$ [m/z 311.13207 $(M + H)^+$]. The IR spectrum of **1** indicated the presence of an ester carbonyl group (1722 cm^{-1}) and an aromatic ring (1600, 1445 cm^{-1}). The ^1H NMR spectrum showed signals due to two phenyl rings (δ_H 7.45–8.07), two oxymethylenes (δ_H 4.79, 4.93), an olefinic methine (δ_H 5.86, t, J = 6.9 Hz), and a singlet methyl group (δ_H 1.85). In the COSY spectrum, the olefinic methine proton correlated with the oxymethylene signal at δ 4.93. The ^{13}C NMR spectrum displayed 19 signals ascribable to 12 aromatic carbons, two ester carbonyls (δ_C 166.2, 166.5), a double bond (δ_C 121.9, 136.1), two oxymethylenes (δ_C 61.1, 69.0), and a methyl carbon (δ_C 14.1) (Table 1). These assignments were

Received: April 29, 2012
Published: June 7, 2012

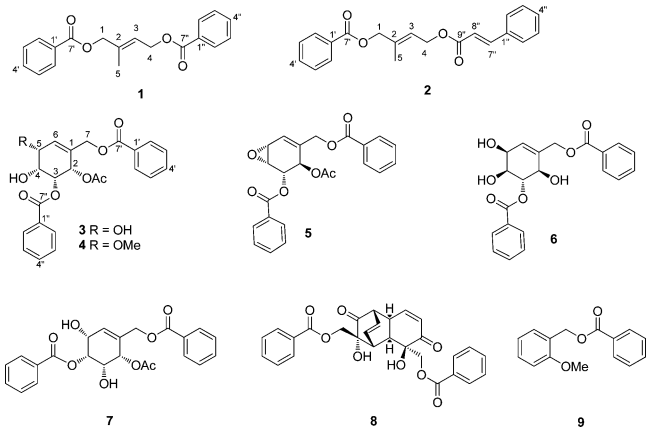

Table 1. ^{1}H and ^{13}C NMR Spectroscopic Data of Compounds 1 and 2 (400 MHz for ^{1}H, 100 MHz for ^{13}C, $CDCl_3$)

	1		2	
position	δ_C	δ_H (J in Hz)	δ_C	δ_H (J in Hz)
1	69.0	4.79, s	68.7	4.68, s
2	136.1		136.2	
3	121.9	5.86, t (6.9 Hz)	121.9	5.82, t (6.9 Hz)
4	61.1	4.93, d (6.9 Hz)	61.3	4.92, d (6.9 Hz)
5	14.4	1.85, s	14.5	1.86, s
1′	130.1		130.3	
2′, 6′	128.4	8.07, t (7.7 Hz)	129.8	8.06, d (7.3 Hz)
3′, 5′	129.7	7.45, m	129.0	7.44, m
4′	133.0	7.56, m	133.1	7.55, m
7′	166.2		166.6	
1″	130.2		134.4	
2″, 6″	128.4	8.07, t (7.7 Hz)	128.5	7.55, m
3″, 5″	129.7	7.45, m	128.2	7.39, m
4″	133.1	7.56, m	130.5	7.39, m
7″	166.5		145.4	7.73, d (16.0 Hz)
8″			117.8	6.49, d (16.0 Hz)
9″			166.7	

supported from the HMQC and HMBC spectra (Figure 1a). The aromatic protons at δ_H 8.07 (2′,6′, 2″,6″) gave HMBC

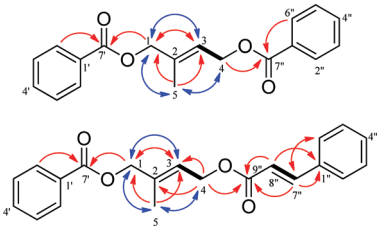

Figure 1. Connectivities (bold line) deduced from the COSY and HMQC spectra, HMBC correlations (red →), and NOESY correlations (blue ↔) for compounds **1** (top) and **2** (bottom).

correlations to two carbonyl carbons, suggesting the presence of two benzoyl groups. These benzoyl groups were deduced to be at C-1 and C-4 on the basis of HMBC correlations observed from H_2-1 to C-7′ and from H_2-4 to C-7″ (Figure 1a). A methyl singlet H_3-5 gave HMBC correlations with an oxymethylene carbon at δ_C 69.0 (C-1), a quaternary olefinic carbon at δ_C 136.1 (C-2), and an olefinic carbon at δ_C 121.9 (C-3), suggesting the location of a methyl group to be at C-2. In the NOESY spectrum, correlations were observed between H-1/H-3, H-1/H-5, and H-5/H-4, suggesting the *E* geometry between C-2 and C-3 (Figure 1a). Therefore, the structure of uvaridacane A (**1**) was assigned as (*E*)-2-methylbut-2-ene-1,4-diyl dibenzoate.

Uvaridacane B (**2**) was isolated as a white, amorphous solid. Its molecular formula was deduced by HRFABMS to be $C_{21}H_{20}O_4$. The ^{1}H NMR data of **2** were similar to those of **1** except for the presence of additional signals due to *trans*-olefinic protons at δ_H 6.49 (d, J = 16 Hz) and δ_H 7.73 (d, J = 16 Hz). The ^{13}C NMR spectrum also showed the presence of two additional carbons at δ_C 117.8 and 145.4 (Table 1). Therefore, the presence of a cinnamoloxy group instead of one of the benzoyl groups in **1** was assumed. The location of the cinnamololoxy group was confirmed to be at C-4 on the basis of the HMBC spectrum (Figure 1b). In the NOESY spectrum, similar correlations were observed between H-1/H-3, H-1/H-5, and H-5/H-4, suggesting the *E* geometry between C-2 and C-3 (Figure 1b). Therefore, the structure of uvaridacane B (**2**) was determined as (*E*)-2-methyl-4-((*E*)-3-phenylprop-2-enoyloxy)-but-2-enyl benzoate.

Uvaridacol A (**3**) was obtained as a white, amorphous solid, $[\alpha]^{23}_D$ −43.5. The molecular formula of **3** was established as $C_{23}H_{22}O_8$ by HRFABMS. The IR spectrum of **3** showed the absorptions of an ester carbonyl (1720 cm^{-1}). In the ^{1}H NMR spectrum, signals were displayed due to four oxymethines (δ_H 4.14, H-4; 4.47, H-5; 5.72, H-2; 5.50, H-3), an oxymethylene (δ_H 4.83, H-7), and an olefinic methine (δ_H 6.18, H-6) together with those for one acetyl and two benzoyl groups (Table 2). The ^{13}C NMR spectrum showed the signals due to 23 carbons that could be ascribable to five oxygenated sp^3 carbons (δ_C 64.3, 69.2, 68.1, 71.8, and 73.2), two olefinic carbons (δ_C 131.0 and 131.6), two benzoyl groups, and an acetyl group (Table 3). The ^{1}H−^{1}H COSY and HMQC spectra revealed the partial connectivity (bold line) of C-2−C-3−C-4−C-5−C-6, which were connected further on the basis of the long-range HMBC correlations (Figure 2a). Thus, in the HMBC spectrum of **3**, the oxymethylene proton at δ_H 4.83 (H_2-7) showed long-range correlations with the oxymethine carbon at δ_C 68.1 (C-2), the olefinic methine carbon at δ_C 131.6 (C-6), and the quaternary olefinic carbon at δ 136.3 (C-1), suggesting the connectivity of C-2, C-6, and C-7 via the quaternary carbon C-1. The locations of the two benzoyl groups were determined to be at C-3 and C-7 on the basis of the correlations between the ester carbonyl carbon at δ_C 166.4 (OCO-3) and the protons at δ_H 8.02 (H-2″,6″) and 4.14 (H-3) and between the ester carbonyl carbon at δ_C 166.0 (OCO-7) and the protons at δ_H 7.97 (H-2′,6′) and 4.83 (H-7). In contrast the location of the acetyl group was determined to be at C-2 on the basis of the correlations of the ester carbonyl carbon (δ_C 169.9, OCO-2) with the protons at δ_H 5.5 (H-2) and the acetyl methyl proton at δ_H 2.07 (Figure 2a). The relative configuration of **3** was assigned on the basis of the NOESY correlations and the coupling constant data. The NOESY correlations between H-2/H-3 and H-3/H-4 (Figure 2b) and the coupling constants $J_{2,3}$ = 3.7 Hz and $J_{3,4}$ = 1.8 Hz (Table 2) indicated a *cis* relationship between H-2, H-3, and H-4. Furthermore, the NOESY correlations between H-4/H-5 and H-3/H-5 suggested that H-3 and H-5 are oriented axially on the same side. Uvaridacol A (**3**) showed a negative Cotton effect ($[\theta]_{242}$ −12 387) due to exciton chirality (Figure 2b),[21,22] suggesting the spatial orientation of two benzoates at C-3 and C-7 to be in a counterclockwise fashion.[22] Therefore, the

dx.doi.org/10.1021/np300295h | J. Nat. Prod. 2012, 75, 1177−1183

Table 2. ^{1}H NMR (400 MHz, $CDCl_3$) Spectroscopic Data of Compounds 3−7

position	3	4	5	6	7
2	5.72, d (3.7 Hz)	5.86, d (5 Hz)	6.14, dd (8.7, 1.8 Hz)	4.64, d (9.2 Hz)	5.59, d (4.58 Hz)
3	5.5, dd (1.8, 3.7 Hz)	5.51, dd (5.0, 2.3 Hz)	5.52, dd (8.7, 0.9 Hz)	4.15, t (9.2 Hz)	4.33, br s
4	4.14, dd (6.9, 1.8 Hz)	4.29, dd (5.95, 2.3 Hz)	3.80, dd (4.1, 0.9 Hz)	5.3, dd (9.2, 6.4 Hz)	5.3, dd (6.4, 2.5 Hz)
5	4.47, d (6.9 Hz)	4.01, m	3.56, t (4.1 Hz)	4.57, d (6.4 Hz)	4.69, dd (2.5, 3.2 Hz)
6	6.18, br s	6.22, d (1.8 Hz)	6.27, br s	5.94, br s	6.16, d (3.21 Hz)
7	4.83, s	4.85, s	4.83, d (13.3 Hz)	4.84, d (13.7 Hz)	4.88, m
			4.89, d (13.3 Hz)	5.15, d (13.7 Hz)	
OBz-7					
2′, 6′	7.97, d (7.8 Hz)	8.01, t (7.3 Hz)	8.03, d (7.8, 0.9 Hz)	8.07, m	7.46, m
3′, 5′	7.41, m	7.42, m	7.43, m	7.44, m	7.59, m
4′	7.56, d (6 Hz)	7.56, q (7.8 Hz)	7.57, m	7.58, m	8.06, m
	OBz-3	*OBz-3*	*OBz-3*	*OBz-3*	*OBz-4*
2″, 6″	8.02, d (7.8 Hz)	8.01, t (7.3 Hz)	8.08, d (7.3, 1.4 Hz)	8.07, m	7.46, m
3″, 5″	7.41, m	7.42, m	7.43, m	7.44, m	7.59, m
4″	7.56, d (6 Hz)	7.56, q (7.8 Hz)	7.57, m	7.58, m	8.06, m
2-OCO$\underline{CH_3}$	2.07	2.04, s			2.11, s
OCH_3		3.55, s			

Table 3. ^{13}C NMR (100 MHz, $CDCl_3$) Spectroscopic Data of 3−7

position	3	4	5	6	7
1	131.0	132.4	138.3	136.1	131.4
2	68.1	67.8	68.9	59.9	70.8
3	73.2	73.3	74.8	74.4	69.4
4	71.8	69.3	52.4	78.8	76.1
5	69.2	77.7	48.6	70.2	66.8
6	131.6	128.3	123.8	126.1	130.7
7	64.3	64.3	63.2	63.9	64.3
OBz-7					
1′	129.1	129.3	129.3	129.3	129.4
2′, 6′	129.7	129.9	129.8	129.9	129.7
3′, 5′	128.5	128.5	128.6	128.6	128.5
4′	133.3	133.5	133.4	133.5	133.3
7′	166.0	165.9	166.0	166.6	166.1
	OBz-3	*OBz-3*	*OBz-3*	*OBz-3*	*OBz-4*
1″	129.6	128.6	129.6	129.6	129.7
2″, 6″	129.9	129.7	130.0	130.0	129.9
3″, 5″	128.5	128.4	128.7	128.6	128.6
4″	133.6	133.2	133.6	133.6	133.6
7″	166.4	166	166.4	167.3	166.8
OAc-2					
OCO$\underline{CH_3}$	20.8	20.8	20.7		20.9
O$\underline{CO}CH_3$	169.9	169.9	169.9		170.9
O$\underline{CH_3}$		57.7			

absolute configuration of uvaridacol A (**3**) was proposed as 2*S*, 3*R*, 4*R*, and 5*R*.

The ^{1}H and ^{13}C NMR spectra of uvaridacol B (**4**) closely resembled those of **3**, except for the presence of an additional signal due to an *O*-methyl group (δ_H 3.55; δ_C 57.7) (Table 2). The HMBC analysis indicated the *O*-methyl group to be at C-5. Uvaridacol B (**4**) showed similar NOESY correlations to **3** and displayed a negative Cotton effect ($[\theta]_{242}$ −10 176). Therefore, the absolute configuration of **4** was concluded to be the same as uvaridacol A (**3**).

Uvaridapoxide A (**5**) was isolated as a white, amorphous solid. The ^{1}H and ^{13}C NMR spectra of **5** were found to closely resemble those of **3** and showed the presence of four oxymethines, an oxymethylene, an olefinic proton, and signals for two benzoyl moieties and one acetyl group. However, the HRFABMS indicated the molecular formula to be $C_{23}H_{20}O_7$, ascribable to the loss of H_2O when compared with **3**. Therefore, the presence of an epoxide was assumed. The upfield shift of the ^{13}C NMR signals of C-4 (δ_C 52.4) and C-5 (δ_C 48.6) indicated that **5** contains this epoxide unit at C-4 and C-5 instead of hydroxy substituents as in **3** (Table 3). The locations of the acetyl and benzoyl substituents were determined to be at C-2 and C-3 from the HMBC spectrum (Figure 2c). The relative configuration was proposed by analysis of coupling constants (Table 2) and NOESY correlations (Figure 2d). In contrast to **3**, uvaridapoxide A (**5**) showed a larger coupling constant between H-2/H-3 ($J_{2,3}$ = 8.7 Hz), indicating their *trans* relationship, while H-3, H-4, and H-5 have similar *cis* relationships to that of **3**. Uvaridapoxide A (**5**) showed a negative Cotton effect ($[\theta]_{239}$ −7658), suggesting the spatial orientation of two benzoates at C-3 and C-7 to be in a counterclockwise orientation.[22] Therefore, the absolute configuration of **5** was established as 2*R*, 3*R*, 4*R*, and 5*R*.

The ^{1}H and ^{13}C NMR spectra of uvaridacol C (**6**) also closely resembled those of **3** (Table 2), but they were characterized by the absence of signals due to the acetyl group of **3**. Analysis of the HMBC spectrum (Figure 2e) indicated the presence of benzoyl substituents at C-3 and C-7, the same as in **3**. However, the larger coupling constant (J = 9.2 Hz) indicated the *trans* relationships between H-2/H-3 and H-3/H-4 and a *cis* relationship between H-4/H-5 (J = 6.4 Hz), which was supported by NOESY correlations between H-2/H-4 and H-4/H-5 (Figure 2f). The absolute stereochemistry of uvaridacol C (**6**) was established as 2*R*, 3*S*, 4*S*, and 5*S* from the negative Cotton effect in the CD spectrum ($[\theta]_{242}$ −10254).

Uvaridacol D (**7**) was obtained as a white, amorphous solid. The ^{1}H and ^{13}C NMR data of **7** closely resembled those of **3** and displayed signals due to two benzoyl groups, an acetyl group, four oxymethines, one oxymethylene, and an olefinic proton. However, there was evidence of an upfield shift of H-3 (δ_H 5.50, **3**) to δ_H 4.33 and a downfield shift of H-4 (δ_H 4.14, **3**) to δ_H 5.3 in **7**. Therefore, a hydroxy at C-3 and a benzoyloxy at C-4 were assumed, which was confirmed from the HMBC spectrum. The relative configuration of **7** was also similar to that of **3** from the NOESY and coupling constant analysis (Table 2). Uvaridacol D (**7**) displayed a negative Cotton effect

dx.doi.org/10.1021/np300295h | *J. Nat. Prod.* 2012, 75, 1177−1183

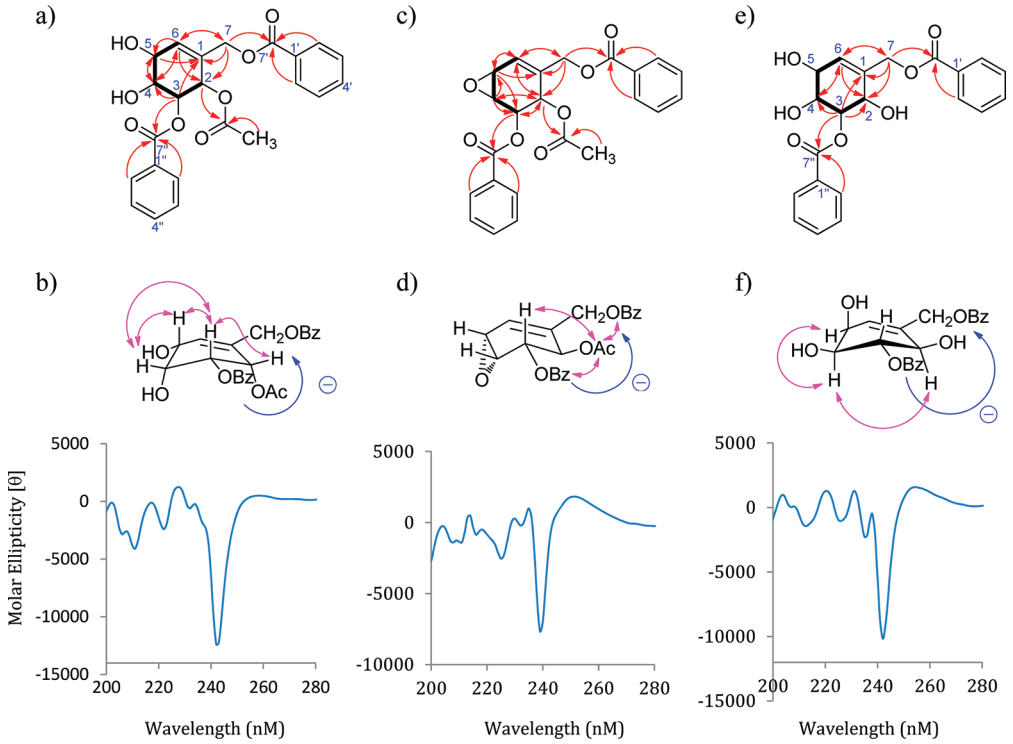

Figure 2. Connectivities (bold line) deduced by the COSY and HMQC spectra and HMBC correlations (red →), NOESY correlations (magenta ↔), exciton chirality (blue →), and CD spectra for compounds **3** (a, b), **5** (c, d), and **6** (e, f).

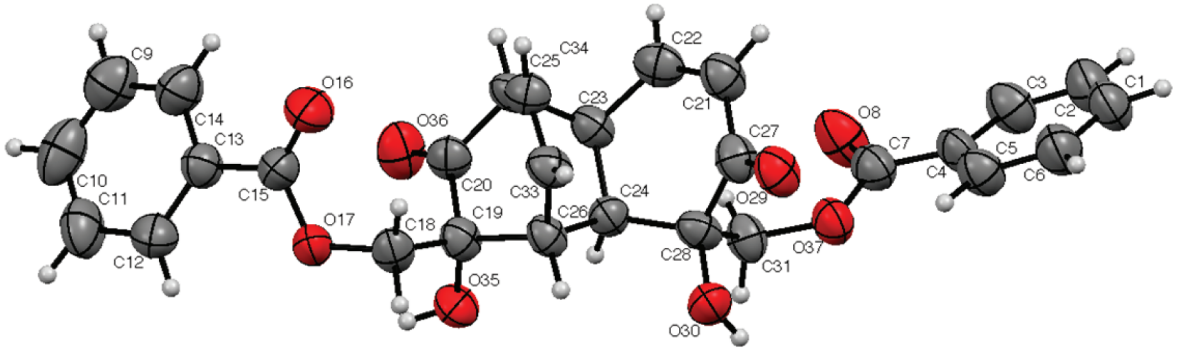

Figure 3. ORTEP diagram of (+)-grandifloracin (**8**).

in its CD spectrum ($[\theta]_{211}$ −19 264) (see Supporting Information Figure S16), attributable to exciton coupling between the benzoyl group at C-4 and the allylic benzoate.[21] Thus, the absolute configuration of **7** was concluded to be 2*S*, 3*S*, 4*R*, and 5*R*.

Grandifloracin (**8**) was isolated as a white, amorphous solid. Its molecular formula was determined by HRFABMS as $C_{28}H_{24}O_8$. The ^{1}H and ^{13}C NMR data (Supporting Information) matched with those for (−)-grandifloracin.[23] However, **8** showed a positive specific rotation of +5.8, similar to the synthesized (+)-grandifloracin recently reported by Lewis et al.[24] Grandifloracin (**8**) was recrystallized in acetone and methanol (1:1) at −30 °C for 10 days to obtain colorless needle cyrstals. The single crystal was subjected to single-crystal X-ray analysis (Figure 3). The crystal structure, together with comparison of the circular dichroism spectrum (Figure 4) of **8** with that of synthetic (+)-grandifloracin,[24] established unambiguously the absolute stereochemistry of **8**, as shown in Figure 3. This is the first time that (+)-grandifloracin (**8**) has been isolated from a natural source.

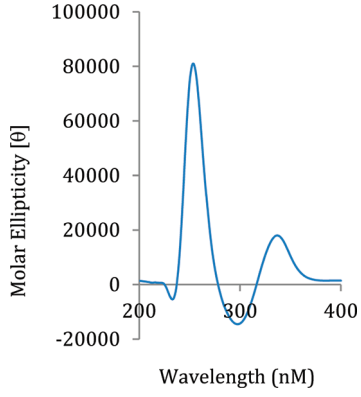

Figure 4. Circular dichroism spectrum of (+)-grandifloracin (**8**) in ethanol.

dx.doi.org/10.1021/np300295h | *J. Nat. Prod.* 2012, 75, 1177−1183

The known compound *o*-methoxybenzoyl benzoate (**9**) was identified by comparison of its spectroscopic data with those published in the literature.[25]

All of the isolated compounds except for **7**[26] were tested for their cytotoxic activity against a panel of four human pancreatic cancer cell lines (PANC-1, PSN-1, MIAPaCa-2, and KLM-1) in normal nutrient-rich medium (DMEM or RPMI) and nutrient-deprived medium (NDM), utilizing an antiausterity strategy.[27] Compounds possessing cytotoxicity in NDM without toxicity in DMEM are considered to be preferentially cytotoxic agents (antiausterity agents). Human pancreatic tumors are hypovascular in nature.[28] However, these tumor cells have an inherent tolerance to nutrition starvation, enabling them to survive under critically low nutrient conditions in the tumor microenvironment.[29] The discovery of agents that preferentially retard this tolerance of nutrient starvation is a novel approach in anticancer drug discovery.[12,13] Among the test compounds, **1**−**6** exhibited mild preferential cytotoxicity against all the lines, with PC_{50} values ranging from 100 to 200 μM (Table 4), while

Table 4. Preferential Cytotoxic Activities (PC_{50}, μM)[a] of Compounds 1−9[b]

	cell lines			
compound	PANC-1	PSN-1	MIA PaCa-2	KLM-1
1	72.3	96.5	56.3	122
2	134	143	57.8	>200
3	102	173	192	83.0
4	69.8	158	147	>200
5	112	80.1	100	159
6	72.9	152	115	–[b]
8	14.5	32.6	17.5	32.7
9	137	185	131	>200
arctigenin[c]	1.7	1.9	0.67	1.5
gemcitabine[d]	>200	>200	>200	>200

[a]Concentration at which 50% of cells were killed preferentially in nutrient-deprived medium (NDM) without causing toxicity in nutrient-rich medium (DMEM). [b]**7** was not tested due to the small amount isolated. [c]Positive control. [d]Clinically used anticancer drug for the treatment of pancreatic cancer.

(+)-grandifloracin (**8**) displayed the most potent activity against the PANC-1 (PC_{50}, 14.5 μM), PSN-1 (PC_{50}, 32.6 μM), MIA PaCa-2 (PC_{50}, 17.5 μM), and KLM-1 (32.7 μM) cell lines in a concentration-dependent manner (see Supporting Information Figure S1). (+)-Grandifloracinn (**8**) induced distinct morphological alterations of PANC-1 cells such as rounding of cells, plasma membrane rupture, and loss of cellular contents to the medium (Figure 5). Arctigenin, an antiausterity strategy-based anticancer agent,[12] was used as a positive control and displayed the most potent preferential cytotoxicy against all the tested cell lines (Table 4). In contrast, gemcitabine, a clinically used anticancer drug for the treatment of pancreatic cancer,[30] was virtually inactive in both NDM and DMEM. Therefore, (+)-grandifloracin (**8**) is an interesting antiausterity candidate for further study.

EXPERIMENTAL SECTION

General Experimental Procedures. Optical rotations were measured on a JASCO P2100 digital polarimeter. CD measurements were carried out on a JASCO J-805 spectropolarimeter. IR spectra were measured with a JASCO FT/IR-460 Plus spectrophotometer. NMR spectra were recorded on a JEOL ECX400 Delta spectrometer

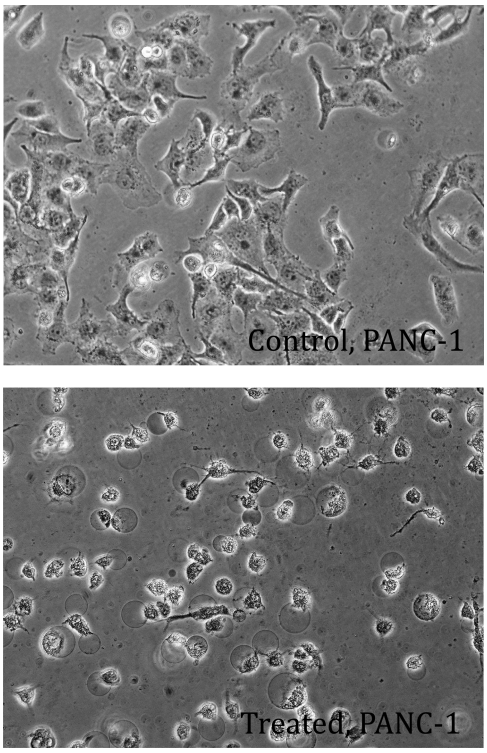

Figure 5. Morphological change induced by (+)-grandifloracin (25 μM) treatment for 24 h against PANC-1 cells.

with TMS as internal standard, and chemical shifts are expressed in δ values. HRFABMS measurements were carried out on a JEOL JMS-AX505HAD mass spectrometer, and glycerol was used as matrix. MPLC was performed with a Büchi MPLC C-605 double gradient pump system with normal-phase silica gel (silica gel 60N, spherical, neutral, 40−50 μm, Kanto Chemical Co., Inc.). Analytical and preparative TLC were carried out on precoated silica gel $60F_{254}$ and RP-$18F_{254}$ plates (Merck, 0.25 or 0.50 mm thickness).

Plant Material. The stems of *Uvaria dac* were collected at Sakaerat Environmental Research Station, Nakhon Ratchasima Province, Thailand, in May 2011. The plant was identified by Dr. Atchara Teerawatananon (Natural Research Division, National Science Museum, Thailand). A voucher specimen (TMPW 27320) was deposited at the Museum for Materia Medica, Institute of Natural Medicine, University of Toyama, Japan.

Extraction and Isolation. The stems of *U. dac* (100 g) were extracted with CH_2Cl_2 under sonication (1 L, 90 min ×3) at room temperature, and the solvent was evaporated under reduced pressure to give a CH_2Cl_2 extract (4.0 g). This extract was chromatographed on silica gel, using a MeOH−CH_2Cl_2 gradient system (Buchi MPLC, C-601/C-605 dual pump), to give nine fractions (fr.1: CH_2Cl_2 eluate, 236 mg; fr.2: 2% MeOH, 90 mg; fr.3: 4% MeOH, 660 mg; fr.4: 6% MeOH, 530 mg; fr.5: 8% MeOH, 13 mg; fr.6: 10% MeOH, 51 mg; fr.7: 12% MeOH, 55 mg; fr.8: 14% MeOH, 102 mg; fr.9: 20% MeOH, 250 mg; fr.10: 30% MeOH, 330 mg). Fractions 1 and 2 were combined and subjected to reversed-phase preparative TLC with CH_3CN−acetone−H_2O (2:2:1) to give **9** (4 mg), and **1** (7 mg)/**2** (5 mg), respectively. Fraction 4 was subjected to reversed-phase MPLC with CH_3CN−acetone−H_2O (1:1:1) to afford four subfractions (fr.4-1, 95 mg; fr.4-2, 80 mg; fr.4-3, 40 mg; fr.4-4, 70 mg). Subfraction 4-1 was purified using reversed-phase preparative TLC with CH_3CN−acetone−H_2O (1:1:1) to furnish three subsubfractions (4-1-1, 10 mg; 4-1-2; 30 mg; 4-1-3, 19 mg), which were then purified by normal-phase preparative TLC with 2% MeOH−CH_2Cl_2 to afford **3** (16 mg) and **5** (40 mg). Fraction 5 was subjected to reversed-phase preparative TLC with CH_3CN−acetone−H_2O (2:2:1) to give **4** (4 mg). Fraction 6 was purified by reversed-phase preparative TLC with CH_3CN−

dx.doi.org/10.1021/np300295h | J. Nat. Prod. 2012, 75, 1177−1183

acetone−H_2O (1:1:1) to give **5** (3 mg), **6** (2.5 mg), **7** (1 mg), and **8** (7 mg), respectively.

Uvaridacane A (1): white, amorphous solid; IR ν_{max} (KBr) 2923, 1722, 1452, 1269, 1110 cm^{-1}; ^1H and ^{13}C NMR, see Table 1; HRFABMS m/z 311.13207 $[M + H]^+$ (calcd for $C_{19}H_{19}O_4$, 311.12834).

Uvaridacane B (2): white, amorphous solid; IR ν_{max} (KBr) 2923, 2361, 1716, 1636, 1451, 1270, 1163 cm^{-1}; ^1H and ^{13}C NMR, see Table 1; HRFABMS m/z 337.14028 $[M + H]^+$ (calcd for $C_{21}H_{21}O_4$, 337.14399).

Uvaridacol A (3): white, amorphous solid; $[\alpha]^{25}_D$ −43.5 (c 1.0, $CHCl_3$); CD (c 2.34 × 10^{-4} M, EtOH) $[\theta]_{242}$ −12 387; IR ν_{max} (KBr) 3396, 1720, 1270, 1112 cm^{-1}; ^1H and ^{13}C NMR, see Tables 2 and 3; HRFABMS m/z 427.13733 $[M + H]^+$ (calcd for $C_{23}H_{23}O_8$, 427.13928).

Uvaridacol B (4): white, amorphous solid; $[\alpha]^{25}_D$−41.5 (c 1.0, $CHCl_3$); CD (c 2.26 × 10^{-4} M, EtOH) $[\theta]_{242}$ −10 176; IR ν_{max} (KBr) 3396, 1720, 1269, 1112 cm^{-1}; ^1H and ^{13}C NMR, see Tables 2 and 3; HRFABMS m/z 441.15287 $[M + H]^+$ (calcd for $C_{24}H_{25}O_8$, 441.15493).

Uvaridapoxide A (5): white, amorphous solid; $[\alpha]^{25}_D$ −25.9 (c 1.0, $CHCl_3$); CD (c 2.32 × 10^{-4} M, EtOH) $[\theta]_{239}$ −76 758; IR ν_{max} (KBr) 3647, 2926, 1722, 1454, 1268, 1108 cm^{-1}; ^1H and ^{13}C NMR, see Tables 2 and 3; HRFABMS m/z 431.10595 $[M + Na]^+$ (calcd for $C_{23}H_{20}O_7Na$, 431.11067).

Uvaridacol C (6): white, amorphous solid; $[\alpha]^{25}_D$ −50.4 (c 1.0, $CHCl_3$); CD (c 2.59 × 10^{-4} M, EtOH) $[\theta]_{242}$ −10 254; IR ν_{max} (KBr) 3420, 2923, 2361, 1718, 1452, 1371, 1269, 1111, 1025 cm^{-1}; ^1H and ^{13}C NMR, see Tables 2 and 3; HRFABMS m/z 385.12697 $[M + H]^+$ (calcd for $C_{21}H_{21}O_7$, 385.12873).

Uvaridacol D (7): white, amorphous solid; $[\alpha]^{25}_D$ −31.5 (c 1.0, $CHCl_3$); CD (c 3.48 × 10^{-4} M, EtOH) $[\theta]_{211}$ −19 264; IR ν_{max} (KBr) 3420, 2923, 2361, 1718, 1452, 1371, 1269, 1111, 1025 cm^{-1}; ^1H and ^{13}C NMR, see Tables 2 and 3; HRFABMS m/z 449.12139 $[M + Na]^+$ (calcd for $C_{23}H_{22}O_8Na$, 287.1283).

(+)-Grandifloracin (8): colorless needle; $[\alpha]^{26}_D$ +5.8 (c 1.0, $CHCl_3$); CD (c 3.48 × 10^{-4} M, EtOH) $[\theta]_{254}$ +80 931; IR ν_{max} (KBr) 3685, 3019, 2400, 1215, cm^{-1}; ^1H and ^{13}C NMR, see Supporting Information; HRFABMS m/z 511.13588 $[M + Na]^+$ (calcd for $C_{28}H_{24}O_8Na$, 511.13687).

X-ray Crystallography of (+)-Grandifloracin (8). $C_{28}H_{24}O_8$, MW = 488.49, colorless needle, monoclinic, primitive, space group $P2_1$ with a = 10.6034(5) Å, b = 6.2661(3) Å, c = 18.0594(8) Å, β = 107.232(3)°, V = 1146.04(9) $Å^3$, Z = 2, D_{calc} = 1.415 g/cm^3, μ(Cu Kα) = 8.688 cm^{-1}, and F(000) = 512. Crystal dimensions: 0.280 × 0.030 × 0.010 mm^3. Independent reflections: 12 736 (R_{int} = 0.0706). The final R_1 = 0.0823, wR_2 = 0.2682, Flack parameter = 0.0(6).

The measurements were done on a Rigaku R-AXIS RAPID diffractometer using filtered Cu Kα radiation by using the ω-scan technique to a maximum 2θ value of 144.2°. The structure was solved by Fourier techniques. The non-hydrogen atoms were refined anisotropically. Hydrogen atoms were refined using the riding model. The absolute structure was deduced on the basis of the Flack parameter, 0.0(6), refined using 1900 Friedel pairs.[31] All calculations were performed using the CrystalStructure crystallographic software package (Rigaku Corporation, 2000−2010, Tokyo, Japan) except for refinement, which was performed using SHELXL-97.[32] Crystallographic data have been deposited at the Cambridge Crystallographic Data Centre. The deposition number of (+)-grandifloracin (**8**) is CCDC 878005. Copies of the data can be obtained free of charge on application to CCDC, 12 Union Road, Cambridge CB2 IEZ, UK. Fax: +44-(0)1223−336033 or e-mail: deposit@ccdc.cam.ac.uk.

Biological Materials. Dulbecco's phosphate-buffered saline (PBS) was purchased from Nissui Pharmaceutical Co., Ltd. (Tokyo, Japan). Dulbecco's modified Eagle's medium (DMEM) and RPMI-1640 were purchased from Wako. Sodium bicarbonate, potassium chloride, magnesium sulfate, sodium dihydrogen phosphate, potassium dihydrogen phosphate, sodium chloride, and phenol red were purchased from Wako. HEPES was purchased from Dojindo (Kumamoto, Japan). Fetal bovine serum (FBS) was from Gibco BRL Products (Gaithersburg, MD, USA). Antibiotic antimycotic solution was from Sigma-Aldrich, Inc. (St. Louis, MO, USA). WST-8 cell counting kit was from Dojindo (Kumamoto, Japan). Cell culture flasks and 96-well plates were obtained from Falcon Becton Dickinson Labware (BD Biosciences, San Jose, CA, USA). Nutrient-deprived medium (NDM) was prepared according to a previously described protocol.[12]

Cancer Cell Lines and Cell Culture. The PANC-1 (RBRC-RCB2095), MIA PaCa-2 (RBRC-RCB2094), and KLM-1 (RBRC-RCB2138) human pancreatic cancer cell lines were purchased from Riken BRC cell bank. The PSN-1 cell line was a kind gift from Prof. Hiroyasu Esumi (National Cancer Center Hospital East, Tokyo, Japan). These cell lines were maintained either in standard DMEM (PANC-1 and MIA PaCa-2) or in RPMI-1640 (KLM-1 and PSN-1) with 10% FBS supplement, 0.1% $NaHCO_3$, and 1% antibiotic antimycotic solution.

Preferential Cytotoxic Activity against PANC-1 Cells in Nutrient-Deprived Medium. The in vitro preferential cytotoxicity of the crude extract and the isolated compounds was determined by a previously described procedure with a slight modification.[13] Briefly, human pancreatic cancer cells were seeded in 96-well plates (2 × 10^4/well) and incubated in fresh DMEM or RPMI-1640 at 37 °C under 5% CO_2 and 95% air for 24 h. After the cells were washed with PBS, the medium was changed to serially diluted test samples in either DMEM or NDM with control and blank in each plate. After 24 h incubation, 100 μL of DMEM containing 10% WST-8 cell counting kit solution was added to each well directly. After 3 h incubation, the absorbance at 450 nm was measured (Perkin-Elmer EnSpire multilabel reader). Cell viability was calculated from the mean values of data from three wells by using the following equation:

$$\text{Cell viability (\%)} = [\text{Abs}_{(\text{test sample})} - \text{Abs}_{(\text{blank})}/\text{Abs}_{(\text{Control})} - \text{Abs}_{(\text{blank})}] \times 100\%$$

Morphological Assessment of Cancer Cells. Cells for the morphological change study were seeded in 60 mm dishes (1 × 10^6) and incubated in a humidified CO_2 incubator for 24 h for the cell attachment. The cells were then washed twice with PSB and treated with 25 μM (+)-grandifloracin (**8**) in DMEM, NDM, and the controls. After 24 h incubation, cell morphology was observed using an inverted Nikon Eclipse TS 100 microscope (40× objective) with phase-contrast. Microscopic images were taken with a Nikon DS-L-2 camera directly attached to the microscope.

■ ASSOCIATED CONTENT

Supporting Information

^1H and ^{13}C NMR spectra of compounds **1**−**9**, X-ray data for (+)-grandifloracin (**8**), and preferential cytotoxic activities of isolated compounds against PANC-1, PSN-1, MIA PaCa-2, and KLM-1 cell lines. This material is available free of charge via the Internet at http://pubs.acs.org.

■ AUTHOR INFORMATION

Corresponding Author

*Tel/Fax: +81-76-434-7640. E-mail: suresh@inm.u-toyama.ac.jp.

Notes

The authors declare no competing financial interest.

■ ACKNOWLEDGMENTS

This work was supported by a grant from Toyama Support Center for Young Principal Investigators in Advanced Life Sciences and a Grant-in-Aid for Scientific Research (No. 24510314) from the Ministry of Education, Culture, Sports, Science and Technology (MEXT), Japan.

REFERENCES

(1) Zhou, G. X.; Zhou, L. E.; Chen, R. Y.; Yu, D. Q. *J. Nat. Prod.* **1999**, *62*, 261−264.
(2) Zhou, G. X.; Chen, R. Y.; Yu, D. Q. *J. Asian Nat. Prod. Res.* **1999**, *1*, 227−238.
(3) Hufford, C. D.; Lasswell, W. L., Jr. *J. Org. Chem.* **1976**, *41*, 1297−1298.
(4) Lasswell, W. L., Jr.; Hufford, C. D. *J. Org. Chem.* **1977**, *42*, 1295−1302.
(5) Chantrapromma, K.; Rat, A. P. Y.; Karalai, C.; Lojanapiwatana, V.; Seechamnanturakit, V. *Phytochemistry* **2000**, *53*, 511−513.
(6) Muhammad, I.; Waterman, P. G. *J. Nat. Prod.* **1988**, *51*, 719−724.
(7) Cole, J. R.; Torrance, S. J.; Wiedhopf, R. M.; Arora, S. K.; Bates, R. B. *J. Org. Chem.* **1976**, *41*, 1852−1855.
(8) Dai, Y.; Harinantenaina, L.; Brodie, P. J.; Callmander, M. W.; Randrianaivo, R.; Rakotonandrasana, S.; Rakotobe, E.; Rasamison, V. E.; Shen, Y.; Tendyke, K.; Suh, E. M.; Kingston, D. G. I. *J. Nat. Prod.* **2012**, *75*, 479−483.
(9) Asha, K. N.; Chowdhury, R.; Hasan, C. M.; Rashid, M. A. *Fitoterapia* **2003**, *74*, 159−163.
(10) Nkunya, M. H.; Weenen, H.; Bray, D. H.; Mgani, Q. A.; Mwasumbi, L. B. *Planta Med.* **1991**, *57*, 341−343.
(11) Hufford, C. D.; Lasswell, W. L., Jr. *Lloydia* **1978**, *41*, 156−160.
(12) Awale, S.; Lu, J.; Kalauni, S. K.; Kurashima, Y.; Tezuka, Y.; Kadota, S.; Esumi, H. *Cancer Res.* **2006**, *66*, 1751−1757.
(13) Awale, S.; Nakashima, E. M.; Kalauni, S. K.; Tezuka, Y.; Kurashima, Y.; Lu, J.; Esumi, H.; Kadota, S. *Bioorg. Med. Chem. Lett.* **2006**, *16*, 581−583.
(14) Awale, S.; Miyamoto, T.; Linn, T. Z.; Li, F.; Win, N. N.; Tezuka, Y.; Esumi, H.; Kadota, S. *J. Nat. Prod.* **2009**, *72*, 1631−1636.
(15) Awale, S.; Linn, T. Z.; Li, F.; Tezuka, Y.; Myint, A.; Tomida, A.; Yamori, T.; Esumi, H.; Kadota, S. *Phytother. Res.* **2011**, *25*, 1770−1775.
(16) Awale, S.; Li, F.; Onozuka, H.; Esumi, H.; Tezuka, Y.; Kadota, S. *Bioorg. Med. Chem.* **2008**, *16*, 181−189.
(17) Win, N. N.; Awale, S.; Esumi, H.; Tezuka, Y.; Kadota, S. *Chem. Pharm. Bull.* **2008**, *56*, 491−496.
(18) Win, N. N.; Awale, S.; Esumi, H.; Tezuka, Y.; Kadota, S. *Bioorg. Med. Chem. Lett.* **2008**, *18*, 4688−4691.
(19) Win, N. N.; Awale, S.; Esumi, H.; Tezuka, Y.; Kadota, S. *Bioorg. Med. Chem.* **2008**, *16*, 8653−8660.
(20) Win, N. N.; Awale, S.; Esumi, H.; Tezuka, Y.; Kadota, S. *J. Nat. Prod.* **2007**, *70*, 1582−1587.
(21) Zhang, C. R.; Yang, S. P.; Liao, S. G.; Wu, Y.; Yue, J. M. *Helv. Chim. Acta* **2006**, *89*, 1408−1416.
(22) Harada, N.; Nakanishi, K.; Berova, N. In *Comprehensive Chiroptical Spectroscopy*; Berova, N., Polavarapu, P. L., Nakanishi, K., Woody, R. W., Eds.; John Wiley & Sons, Inc.: New York, 2012; p 115.
(23) Liao, Y. H.; Xu, L. Z.; Yang, S. L.; Dai, J.; Zhen, Y. S.; Zhu, M.; Sun, N. J. *Phytochemistry* **1997**, *45*, 729−732.
(24) Palframan, M. J.; Kociok-Köhn, G.; Lewis, S. E. *Org. Lett.* **2011**, *13*, 3150−3153.
(25) Lasswell, W. L., Jr.; Hufford, C. D. *Phytochemistry* **1977**, *16*, 1439−1441.
(26) Compound **6** was not tested due to the small amount isolated.
(27) Lu, J.; Kunimoto, S.; Yamazaki, Y.; Kaminishi, M.; Esumi, H. *Cancer Sci.* **2004**, *95*, 547−552.
(28) Ghaneh, P.; Kawesha, A.; Evans, J. D.; Neoptolemos, J. P. *J. Hepatobiliary Pancreat. Surg.* **2002**, *9*, 1−11.
(29) Izuishi, K.; Kato, K.; Ogura, T.; Kinoshita, T.; Esumi, H. *Cancer Res.* **2000**, *60*, 6201−6207.
(30) Eltawil, K. M.; Renfrew, P. D.; Molinari, M. *J. Hepatobiliary Pancreat. Surg.* **2012**, *14*, 260−268.
(31) Flack, H. D. *Acta Crystallogr. A* **1983**, *39*, 876−881.
(32) Sheldrick, G. M. *Acta Crystallogr. A* **2007**, *64*, 112−122.